HHS Public Access

Author manuscript

J Air Waste Manag Assoc. Author manuscript; available in PMC 2018 January 01.

Published in final edited form as:

J Air Waste Manag Assoc. 2017 January ; 67(1): 86–95. doi:10.1080/10962247.2016.1230079.

A novel calibration approach using satellite and visibility observations to estimate $PM_{2.5}$ exposures in Southwest Asia and Afghanistan

Shahir Masri, S.D.,

Exposure, Epidemiology, and Risk Program, Department of Environmental Health, Harvard T.H. Chan School of Public Health, Landmark Center West, Room 412-E. 401 Park Drive. Boston, MA 02215

Eric Garshick, M.D.,

Pulmonary, Allergy, Sleep, and Critical Care Medicine Section, Medical Service, VA Boston Healthcare System, Channing Division of Network Medicine, Brigham and Women's Hospital, Harvard Medical School, Boston, MA, USA.

Brent Coull, Ph.D., and

Department of Biostatistics, Harvard T. H. Chan School of Public Health, Boston, MA, USA.

Petros Koutrakis, Ph.D.

Exposure, Epidemiology, and Risk Program, Department of Environmental Health, Harvard T.H. Chan School of Public Health, Boston, MA, USA.

Introduction

In the U.S. and much of Europe, the development of extensive PM monitoring networks has enabled the successful characterization of historic PM exposure over large regions. However, in most countries of the world, monitoring networks do not exist. This lack of quantitative PM exposure information, particularly in Southwest Asia and Afghanistan where PM values are known to be elevated, limits the assessment of potential health effects, both in the native population and in previously deployed military personnel. There are reports of asthma in returning deployers as well as elevated rates of encounters for asthma/COPD and allied conditions relative to soldiers at U.S. bases (Szema et al. 2011; Szema et al. 2010; Abraham et al. 2012; Abraham et al. 2014).

Although several wealthier countries in the region such as Kuwait, Qatar, and the United Arab Emirates have established limited networks for monitoring PM_{10} and several gaseous pollutants since the early 2000s, there are no networks designed to provide comprehensive air pollution data throughout the entire region, as exists in the U.S. and Europe. In several countries, limited $PM_{2.5}$ measurements began only over the last five years and employ sampling methods that are inadequate to collect particles during dust storms, which are common occurrences each year (NRC, 2010).

Correspondence to: Shahir Masri.

In response to concerns about the respiratory effects of deployment in these regions, the Department of Defense (DoD) conducted the Enhanced Particulate Matter Surveillance Program (EPMSP) at military sites during 2006-2007 showing that mean concentrations of particulate matter less than or equal to 2.5 μm in aerodynamic diameter ($PM_{2.5}$) ranged from approximately 35 to 145 μg/m^3 (NRC, 2010). This is considerably higher than the annual national average encountered in the U.S. during the same period (~12 μg/m^3) and exceeds the 1-year Military Exposure Guideline value (15 μg/m^3) set by the U.S. Army Center for Health Promotion and Preventive Medicine (USEPA, 2016). This type information, albeit on a greater spatial and temporal scale, is critical to enabling causal inference.

Sources of PM near military bases in Southwest Asia and Afghanistan include windblown dust and dust storms, as well as local combustion sources such as open-pit refuse burning, compression ignition vehicles, aircraft engines, diesel electric generators, and local industry (IOM, 2011). This mix of pollution sources is different from that encountered in the U.S. and Europe, where most previous health studies have been conducted. Further, PM exposures in this region are orders of magnitude higher than those commonly found in the U.S., and last several months to several years depending on the length and numbers of deployments.

In a recent study, we established the relationship between visibility and $PM_{2.5}$ in Southwest Asian and Afghanistan (Masri et al. 2015). This relationship with visibility is due to the light extinction (scattering and absorption) effects of particles with sizes similar to the wavelengths of visible light, which has been empirically shown in a number of studies (Burt, 1961; Noll et al. 1968; Charlson, 1969; Waggoner and Weiss, 1980; Abbey et al. 1995). Though visibility is a useful surrogate of human exposures to ambient particles, measurements are spatially limited by the number of existing monitoring stations.

An alternate measurement of light extinction by particles in the atmosphere is aerosol optical depth (AOD), collected by satellite. AOD is a vertical integration measure of the total abundance of particles in the entire atmospheric column, in contrast to visibility which is a measure of the particle abundance near the ground. Satellite imagery of the earth's surface and atmosphere represents an important tool for air quality and pollution monitoring due to its extensive spatial coverage and repeated observations. Like visibility, AOD can be used to estimate ground level PM exposure. Our research team has previously developed methods for the application of high-resolution satellite data for exposure assessment and health effects studies (Kloog et al. 2011; Kloog et al. 2012; Lee et al. 2012; Chudnovsky 2013b; Kloog et al. 2014). Such work has enabled the reliable assessment of short- and long-term human exposures to $PM_{2.5}$, allowing for the investigation of both the acute and chronic effects of ambient particles. Application of our exposure estimates include the assessment of the association of $PM_{2.5}$ with both hospital admissions in New England and birth weight for all births in Massachusetts.

In the present study, we conducted a pilot assessment using previously collected AOD and visibility data in Iraq to model $PM_{2.5}$ concentrations. Specifically, we used 1,845 paired daily airport visibility and AOD measurements (1×1 km resolution) collected in Iraq to develop a calibration model that will be used to convert AOD to ground visibility estimates

in the region. Using the relationship between visibility and $PM_{2.5}$ from our previous work in the region, we estimated $PM_{2.5}$ over an area of approximately 17,000 km^2 in Iraq during a period of two years (2006 - 2007).

Methods

Iraq is a large desert country located at the northern end of the Persian Gulf, to the west of Iran and east of Syria. The country experiences summers that are hot and dry, extending for roughly four months, from June to September, and with temperatures often in excess of 38° (~100°F). Winters are long but mild, lasting from December to March, and with nighttime temperatures typically above freezing. Precipitation and humidity are low, with annual precipitation averaging less than 25 cm across most of the country. The general region is subject to Shamal winds, which generate intense dust storms, usually during the summer months of June and July (NOAA, 2009).

We selected a region in Iraq of approximately 17,000 km^2 that includes Bagdad and Joint-Base-Balad (JBB). This region was selected because of its high yet variable air pollution levels and the presence of U.S. military personnel, which gives relevance to understanding such variability and pollution concentrations (IOM, 2011). Additionally, the region is sufficiently large to encompass low population desert areas with fewer pollution sources, and in turn enable an understanding of the $PM_{2.5}$ in the region.

Aerosol Optical Depth

AOD measurements were collected by the Moderate Resolution Imaging Spectroradiometer (MODIS), which sits on two Earth Observing System (EOS) satellites launched by the National Aeronautic and Space Administration (NASA); namely Terra, launched in 1999, and Aqua, launched in 2002. The MODIS satellite provides daily AOD measurements for the entire Earth. Daily observations were retrieved for the years 2006 and 2007 for the entire area of Iraq. Recently, NASA developed a new algorithm, Multi-Angle Implementation of Atmospheric Correction (MAIAC), to process MODIS data. MAIAC retrieves aerosol parameters over land at a high resolution of 1×1 km, as compared to previously reported 10 km. Our research team has evaluated the first and second generation of MAIAC products and have applied them successfully to assess $PM_{2.5}$ exposures and health effects in New England (Fleisch et al. 2014). From our analyses, we have determined that MAIAC data can also be used for arid (desert) environments with high surface reflectance such as Iraq.

Visibility Data

Visibility data were obtained from the U.S. Air Force 14th Weather Squadron and included seven sites across the study region and period. Visibility was measured continuously using either an AN/FMQ-19 Automatic Meteorological Station or a TMQ-53 Tactical Meteorological Observing System, and was reported hourly. Most sensors measure visibility from approximately 400 to 9,999 m. Maximum measurements exceeding this typical upper limit become less accurate, which can introduce error and affect the relationship between visibility and atmospheric particle mass. Measurements greater than this cutoff were therefore truncated to 9,999 m in this analysis. In order to generate daily averages for use in

model calibration, we averaged hourly measurements over 24-hour periods that coincided with daily AOD measurements. Rain and near-saturation periods, when relative humidity ≥98%, were not included in the analysis. However, since this region is arid with low rainfall, these conditions were observed for only a small fraction of days (~4%).

Statistical Approach

To calibrate a model that uses AOD to predict visibility, we matched each of seven visibility-monitoring stations with a corresponding 1×1 km AOD grid cell. Paired measurements were matched by selecting the AOD grid cell that contained the corresponding visibility station. In contrast to studies that use coarse resolution satellite data, our use of high resolution (1×1 km) AOD measurements enabled more precise pairing of AOD with visibility, and therefore more accurate calibration of the AOD-visibility relationship. In total, 1,845 paired AOD-visibility observations were used for model calibration, spanning a two-year period from January 2006 to Dec 2007. The locations of visibility monitoring stations are depicted in Figure 1. Visibility monitoring sites used in model calibration were located in both rural and urban areas, and contributed variable amounts of data for model calibration (not all stations contained 365 daily observations). In terms of total data used in model calibration, however, an approximately equal amount of rural (45%) and urban (55%) observations were represented. Using our AOD-visibility matched measurements, we applied a mixed-effects model using AOD measurements as predictors to establish a relationship between visibility and AOD.

In order to estimate visibility and convert these estimates to $PM_{2.5}$ in each grid cell on each day, we conducted the prediction process in four stages. Before presenting each stage, we will first summarize the stages here. The Stage 1 model calibrates the AOD grid-level observations to the visibility monitoring data collected within 1 km of an AOD reading by regressing visibility monitoring data on AOD values. Since the relationship between AOD and visibility varies day to day (due to differences in mixing height, relative humidity, particle composition, vertical profiles, etc.) this calibration is performed on a daily basis. In Stage 2 we predict visibility concentrations in grid cells where no visibility monitoring exists but with available AOD measurements using the Stage 1 AOD-visibility relationship. This is achieved by applying the prediction equation obtained from the model fit in Stage 1 to these additional AOD values. In Stage 3, we fit a model using predicted visibility from Stage 2 and spatial associations among visibility values on a given day to estimate visibility in cells where both visibility and AOD data is missing. To convert visibility to $PM_{2.5}$ concentrations in each grid cell, Stage 4 then applies coefficients of the relationship between visibility and $PM_{2.5}$ demonstrated from previous work in the region. The four stages are applied to data at the 1 × 1 km grid cell level.

Stage 1

To predict visibility, we fit the following mixed-effects multiple linear regression model:

$$VIS_{ij} = (\alpha + u_j) + \left(\beta_{1AOD} + v_{jAOD}\right)(1/AOD)_{ij} + \varepsilon_{ij}$$
$$\left(u_j\ v_{jAOD}\right) \sim \mathrm{N}\left[(0 \quad 0), \Sigma\right] \qquad (1)$$

where, VIS_{ij} is the visibility measured at site i corresponding to grid cell i on day j; α and u_j are the fixed and day-specific random intercepts, respectively; AOD_{ij} is the AOD value in the grid cell i on day j; β_{1AOD} and v_{jAOD} are the fixed and day-specific random slopes for AOD; $\varepsilon_{ij} \sim N(0, \sigma^2)$ is the error term at site i on day j; and Σ is the variance-covariance matrix for the day-specific random effects.

In this model, inverse AOD was used since AOD is a measure of particles in the atmospheric column, and the functional relationship between atmospheric particulate and visibility is known to be inverse. That is, as particulate concentrations increase (increasing AOD), visibility decreases. Since the relationship of AOD and visibility (surrogate for $PM_{2.5}$) varies day to day, calibration was performed on a daily basis. Other covariates were tested such as season, weekday/weekend, elevation, wind direction, precipitation, and numerous land use variables (e.g., distance to oil fields, town centers, waterbodies, etc.), which were obtained either from the U.S. Air Force or ArcGIS®. Such terms, however, were either not statistically significant or did not improve model performance. After developing the model, predicted and measured daily visibility values were then assessed on a scatter plot.

For validation, we performed a 10-fold cross validation analysis. This was accomplished by randomly sorting our dataset and dividing it into 10 splits. The model, fit to 90% (nine splits) of the visibility data, was then used to predict visibility in the remaining 10% (one split). This process was repeated 10 times, with each iteration holding out a new 10% split of data. Model performance was examined by comparing predicted and measured visibility for each of the 10 CV trials. Specifically, R^2 values were computed and tabulated for each trial along with the square root of the mean squared prediction errors (RMSPE). Further, we estimated the temporal R^2 by regressing the predicted $delta\,VIS_{ij}$ against the measured $delta\,VIS_{ij}$, where predicted $delta\,VIS_{ij}$ is the difference between the predicted VIS_{ij} in a site corresponding to cell i on day j and its overall mean, and measured $delta\,VIS_{ij}$ is defined similarly for the measured values. Lastly, we estimated the spatial R^2 by regressing the site-specific predicted VIS means on the measured one.

Stage 2

To predict visibility for grid cells containing AOD but no visibility measurements, we used the calibrated coefficients and parameters fitted in Stage 1. This resulted in two yearly sets of visibility predictions for all day-AOD cell available combinations yet still no predictions in day-cell combinations with missing AOD data.

Stage 3

To predict visibility for grid cells that contain neither visibility nor AOD measurements (often due to cloud cover), we used the output of Stage 1 (visibility predictions) to predict daily visibility for all grid cells in the study domain. Specifically, we fit a Generalized

Additive Mixed Model (GAMM) with a smooth function of latitude and longitude (using the grid cell centroids) and a random intercept for each cell. This is similar to other established interpolation techniques, such as universal kriging, that use nearby grid cells to fill missing points. However, in our analysis we also regressed the daily visibility predictions on the average of those measured at the monitoring stations located within our study region. To allow for the visibility spatial patterns to vary with time, we fit a separate spatial surface for each two-month period of each year. This enabled our model to incorporate additional information about visibility values that classic interpolation techniques do not utilize. Specifically, we fit the following semiparametric regression model:

$$PredVIS_{ij} = (\alpha + u_i) + (\beta_1 + v_i)\,(MVIS_{ij}) + s(X_i, Y_i)_{k(j)} + \varepsilon_{ij}$$
$$(u_i\ v_i) \sim [(0 \quad 0), \Omega_\beta] \qquad (2)$$

where $PredVIS_{ij}$ is the Stage 2 predicted visibility at grid cell i on a day j; $MVIS_{ij}$ is the mean of visibility values monitored at the sites in our study region for cell i on a day j; α and u_i are the fixed and grid-cell specific random intercepts, respectively; β_1 and v_i are the fixed and random slopes, respectively; X_i,Y_i are the latitude and longitude, respectively, of the centroid of grid cell i; and, $s(X_i,Y_i)_{k(j)}$ is a smooth function of location (modeled by thin plate splines) specific to the two-month period k(j) in which day j falls, thus a separate spatial smooth was fit for each two-month period.

As with model calibration, visibility predictions here were validated using 10-fold cross validation. In this case, we randomly selected 10% of the data across all visibility monitoring sites (seven grid cells) to leave out of the Stage 3 model predictions. The 90% remaining data from the seven sites was then combined with all data from all other grid cells. This combined data set was then used to predict the 10% left out data from the seven monitoring sites. This process was repeated 10 times, with each iteration holding out a new 10% split of monitoring data. Goodness of fit and model bias were then assessed by regressing predicted and measured visibility at the 10% left out data, and calculating the corresponding R^2 values for each of the 10 separate iterations. As with Stage 1, temporal and spatial cross validation was also applied.

Stage 4

In our previous work, daily-integrated $PM_{2.5}$ concentration data collected at several monitoring sites in Kuwait during the period 2004-2005 was used to calibrate a model for the relationship between $PM_{2.5}$ and visibility, with relative humidity as a covariate (Masri et al. 2015). This study produced $PM_{2.5}$ predictions that correlated well with observed averages (r2=0.84) and performed well through 10-fold internal cross validation. Further, results from mixed model regression in this study demonstrated that predictability did not depend on location within the region. To convert visibility to spatially- and temporally-resolved $PM_{2.5}$ concentrations in the current study, we used the calibration equation coefficients generated from this previous work. The prediction equation is as follows:

$$PredPM_{2.5ij}=\gamma_o+\gamma_v\left(\frac{1}{PredVIS_{ij}}\right)+\gamma_m\left(RH^2\right) \quad (3)$$

where $PredPM_{2.5ij}$ is the predicted $PM_{2.5}$ for cell i on a day j; $PredVIS_{ij}$ is the daily visibility predicted for cell i on a day j; RH^2 is the square of relative humidity for cell i on day j; γ_o, γ_v, and γ_m are the coefficients estimated from our previous analysis, which are equal to +39.3691, +732372, and −0.00319, respectively (Masri et al. 2015). Grid- and day-specific $PM_{2.5}$ predictions over varying periods were then calculated and a map of grid-cell specific averaged $PM_{2.5}$ estimates over the entire study period was projected onto a map for visual representation.

Results

Figure 2 depicts the relationship between predicted and measured daily visibility. Each point represents a single day for a single station within one year. Importantly, there are only 1,845 observations presented in the plot because visibility observations were available for only short periods at some of the visibility stations (not 365 days of the year). Regressing daily visibility resulted in a high r^2 value of 0.87, indicating good model fit.

Table 1 presents results from stage 1 cross validation (CV) analysis. CV trials demonstrated good out-of-sample predictive ability, with a mean out-of-sample R^2 value of 0.71 and range from 0.63 to 0.83. Overall, a significant association was found between visibility and AOD. Table 1 also presents results for spatial and temporal CV analyses. Results for the spatial analysis showed a high mean R^2 of 0.87 (range 0.60-0.98). This demonstrates the ability of the model to predict well from site to site. Results for the temporal analysis showed an R^2 of 0.60 (range 0.51-0.73). The lower temporal R^2 is likely due to our use of only two years of data. Results nonetheless demonstrate that predictions behave similarly to observations over time. Figure 3 shows predicted and measured visibility for each of the 10 CV trials. The resulting plot shows a high R^2 of 0.85, further illustrating the high predictive power of the model.

Table 2 presents results from stage 3 cross validation (CV) analyses after predicting visibility where neither AOD nor visibility measurements are available. CV trials suggested a very good model performance, with a mean out-of-sample R^2 value of 0.84 (range 0.78-0.91). This is a good performance, particularly considering the absence of both AOD and visibility measurements for the days and grid cells being predicted. Table 2 also presents results for spatial and temporal CV analyses. The spatial analysis produced a high mean out-of-sample R^2 of 0.91 (range 0.69-0.99). Results for the temporal analysis were lower, but still good, with a mean out-of-sample R^2 of 0.71 (range 0.56-0.84). Figure 3 shows average predicted and measured visibility for each of the 10 CV trials.

Prediction errors (RMSPE, root mean squared prediction errors) for CV analyses of both models 1 and 2 were low on average (791 and 580 m, respectively), corresponding to an

error of 9 and 7%, respectively, relative to the mean of visibility (~8,500 m) across CV trials. This indicates strong model performance.

Figure 4 illustrates the spatial pattern of $PM_{2.5}$ predictions, with a high resolution of 1×1 km, averaged over the two-year study period from 2006 to 2007. Major roadways as well as the city of Baghdad are labeled. The mean and median predicted $PM_{2.5}$ concentrations for this study area were 45.4 and 39.3 μg/m^3, respectively. The slightly skewed distribution of predicted concentrations is possibly due to episodic dust storms. In general, $PM_{2.5}$ concentrations ranged greatly between grid cells. The interquartile range of mean estimated $PM_{2.5}$ concentrations was 14.6 μg/m^3 (34.2 to 48.8 μg/m^3) with a 10th and 90th percentile of 28.8 and 66.7 μg/m^3, respectively.

As seen in Figure 4, $PM_{2.5}$ predictions are highest in and around Baghdad and Balad as well as along certain roadways, with concentrations in the range of 46.6 to 61.5 μg/m^3. Joint Base Balad (JBB) military base had high $PM_{2.5}$ concentrations, although not as high as those of neighboring city centers.

$PM_{2.5}$ monthly predictions for each of the seven military airport sites and their averages across sites during the 24-month study period are shown in Figure 5. This figure demonstrates that predicted $PM_{2.5}$ varied substantially by month and site. Monthly average predictions ranged from 32.7 to 63.5 μg/m^3, with an overall mean of 45.4 μg/m^3.

When looking at seasonal $PM_{2.5}$ levels over the study period, summer had the highest predicted average, with a concentration of 51.8 μg/m^3. This is consistent with seasonal patterns for this region, in which PM in summer is elevated due to seasonal Shamal winds. Averages across other seasons were markedly lower than summer and comparable to one another, with averages of 41.5, 43.7, and 44.6 μg/m^3 for fall, spring, and winter, respectively. Mean predictions between the two study years were similar, with 2007 having a slightly higher average (47.6 μg/m^3) compared to 2006 (43.3 μg/m^3).

Over the 24-month study period, monthly average predictions across all sites ranged from 29.8 to 69.9 μg/m^3, with a mean and standard deviation of 46.0 and 7.8 μg/m^3, respectively. When assessing inter-site variability for individual months, monthly mean concentrations were somewhat but not highly variable. Inter-site variability for fixed months ranged from 0.60 to 9.9 μg/m^3. For specific months, sites did not deviate greatly from the mean, with a mean standard deviation of 1.4 μg/m^3 across all months. This suggests that location explains approximately 20% of the variability in monthly mean $PM_{2.5}$ estimates observed for the sites in this study. This is shown clearly in Figure 5, where inter-month variability of predicted $PM_{2.5}$ is high, while inter-site variability within individual months is relatively low.

Discussion

In previous studies, the AOD-$PM_{2.5}$ relationship has been calibrated in order to produce spatial $PM_{2.5}$ estimates (Yanosky et al. 2008; Liu et al. 2009; Lee et al. 2011; Kloog et al. 2012). In Southwest Asia and Afghanistan, however, such $PM_{2.5}$ measurements are mostly nonexistent. To overcome this limitation in the current study we employed novel

methodology using readily available airport visibility measurements to calibrate the AOD-visibility relationship and predict visibility over space and time, resulting in monthly average predictions that were highly associated with observed averages (r^2=0.94). In previous work, we established and cross-validated a relationship between visibility and $PM_{2.5}$ in Kuwait. Utilizing this work in the current study, we were able to convert spatial visibility predictions into $PM_{2.5}$ estimates.

Previous studies using satellite observations to predict $PM_{2.5}$ concentrations typically predict with a relatively coarse (10×10 km) spatial resolution and often present moderate predictive power (Lee et al. 2011; Kloog et al. 2012; Yanosky et al. 2008; Liu et al. 2009). A key advantage to our study is the fine 1×1 km resolution of predictions. This helps to reduce exposure error. Additionally, our models yielded high predictive power, in contrast to many other prediction models which assumed that the AOD-$PM_{2.5}$ relationship remains constants over time (Gryparis et al. 2009; Yanosky et al. 2008; Aguilera et al. 2007). These results demonstrate the feasibility of using our methods to assess historic $PM_{2.5}$ concentrations in Southwest Asian and Afghanistan, information that was previously not available.

Multiple means of validating the calibration model were employed in this analysis. Internal cross validation results demonstrated the ability of the model to predict visibility well across randomly divided splits of data, with low prediction errors (~6%) on average. Additionally, roughly equal amounts of rural and urban observations were used in model calibration, which was important given the variability of pollution sources from both land use types.

Given that visibility monitors are restricted to finite maximum readings, a limitation in using visibility measurements is that they are inherently less accurate in cleaner atmospheres. For this reason, it may not be feasible to use visibility as an intermediate to relate AOD with $PM_{2.5}$ mass in regions such as the U.S. where particulate levels are low. In the present study region, this is of little concern since the region is characterized by high concentrations of ambient $PM_{2.5}$ (NRC, 2010). Additionally, use of visibility is particularly advantageous here given the absence of $PM_{2.5}$ samplers in the study area and surrounding region. Through cross-validation, the model predicted well even towards the upper bound of visibility readings. Regarding precipitation, while excluding days with rain could overestimate PM exposure, this was of negligible concern in this study due to the low frequency of rain events in this region.

During the two-year period of this study, average predicted $PM_{2.5}$ was 45.4 $\mu g/m^3$. This estimate places Iraq in roughly the midrange of ambient $PM_{2.5}$ levels relative to other countries in the region. For comparison, the World health Organization (WHO) reported $PM_{2.5}$ in Lebanon (2010) and Saudi Arabia (2011) at 20 and 28 $\mu g/m^3$, respectively, while Iran (2010) and Qatar (2012) had substantially higher reported $PM_{2.5}$ at 102 and 93 $\mu g/m^3$, respectively (WHO, 2014). Similarly, the DOD Enhanced Particulate Matter Surveillance Program reported average $PM_{2.5}$ concentrations ranging from 33 to 117 $\mu g/m^3$ across 15 sites in Southwest Asia and Afghanistan, with an average concentration of approximately 70 $\mu g/m^3$ across all sites (DRI, 2008). The average $PM_{2.5}$ prediction in the current study is similar to that reported in neighboring Jordan (48 $\mu g/m^3$) and Kuwait (45 $\mu g/m^3$) (Brown et al. 2008; WHO, 2014). $PM_{2.5}$ predictions were also the highest during the summer months

mostly due to episodic Shamal winds that generate severe dust storms. This pattern is consistent with previous PM studies in the area, including our previous work in Kuwait (NRC, 2010). In addition, consistency with previously reported measurements reinforces the quality of $PM_{2.5}$ estimates. Annually averaged predictions in this study exceeded EPA (12 $\mu g/m^3$) and WHO (10 $\mu g/m^3$) suggested annual standards.

We examined the spatial patterns of the two-year average $PM_{2.5}$ estimates. Grid cells in and around Baghdad, Joint-Base-Ballad, and major roadways were characterized by the highest estimated $PM_{2.5}$ levels (45-60 $\mu g/m^3$). This is due to the presence of air pollution sources in these areas such as roadway traffic, industry, airports, and residential sources. Military bases often have additional sources from local diesel generators, heavy-duty vehicles, and open-pit waste incineration. Variability between sites was also high, with monthly averages differing by as much as ~30 $\mu g/m^3$ between all sites over all months. Approximately 20% of between-site variability over time was attributable to location, while 80% was attributable to month of year. Importantly, this study focused on a specific region in Iraq over a two-year period. It is likely that the variability in $PM_{2.5}$ estimates would be even greater when assessing a larger geographic area and over a longer period.

At present, very little $PM_{2.5}$ exposure data exists in Southwest Asia and Afghanistan and is not available historically. Our results demonstrate the feasibility of using airport visibility and AOD data calibrated to ground-level $PM_{2.5}$ to estimated exposures in this region.

Acknowledgements

This work was supported by the VA Cooperative Studies Program #595: Pulmonary Health and Deployment to Southwest Asia and Afghanistan, from the United States (U.S.) Department of Veterans Affairs, Office of Research and Development, Clinical Science Research and Development, Cooperative Studies Program. We appreciate the assistance of Mike Hunsucker and Jeff Zautner, 14th Weather Squadron (USAF), Asheville, NC. This publication was also made possible by USEPA grant RD-83479801. Its contents are solely the responsibility of the grantee and do not necessarily represent the official views of the USEPA, U.S. Department of Veterans Affairs, or U.S. Government.

Biography

Shahir Masri is a doctoral of science recently graduated from the Department of Environmental Health, Harvard T. H. Chan School of Public Health, in Boston, MA.

Eric Garshick is a doctor at the in the Pulmonary, Allergy, Sleep, and Critical Care Medicine Section of the V.A. Boston Healthcare System.

Brent Coull is a professor of biostatistics at the Harvard T. H. Chan School of Public Health.

Petros Koutrakis is a professor of environmental sciences at the Harvard T. H. Chan School of Public Health.

References

Abbey D, Ostro BE, Fraser G, Vancuren T, Burchette RJ. Estimating fine particulate less than 2.5 microns in aerodynamic diameter (PM2.5) from airport visibility data in California. J Expo Anal Environ Epidemiol. 1995; 5:161–180. [PubMed: 7492904]

Aguilera I, Sunyer J, Fernández-Patier R, Hoek G, AguirreAlfaro A, Meliefste K, Bomboi-Mingarro MT, Nieuwenhuijsen MJ, Herce-Garraleta D, Brunekreef B. Estimation of outdoor NOx, NO2, and BTEX exposure in a cohort of pregnant women using land use regression modeling. Environ. Sci. Technol. 2007; 42:815–821. doi:10.1021/es0715492.

Brown KW, Bouhamra W, Lamoureux DP, Evans JS, Koutrakis P. Characterization of particulate matter for three sites in Kuwait. J. Air & Waste Manage. Assoc. 2008; 58:994–1003. doi: 10.3155/1047-3289.58.8.994.

Burt EW. A study of the relation of visibility to air pollution. Am Ind Hyg Assoc J. 1961; 2:102–108. doi:10.1080/00028896109343378.

Charlson RJ. Atmospheric visibility related to aerosol mass concentration: review. Environ Sci Technol. 1969; 3:913–918. doi:10.1021/es60033a002.

Chudnovsky A, Tang C, Lyapustin A, Wang Y, Schwartz J, Koutrakis P. A critical assessment of high-resolution aerosol optical depth retrievals for fine particulate matter predictions. Atmos. Chemistry and Physics. 2013; 13:10907–10917. doi:10.5194/acp-13-10907-2013.

Fleisch AF, Gold DR, Rifas-Shiman SL, Koutrakis P, Schwartz JD, Kloog I, Melly S, Coull BA, Zanobetti A, Gillman MW, Oken E. Air pollution exposure and abnormal glucose tolerance during pregnancy: the project viva cohort. Environmental Health Perspectives. 2014; 122:378–383. doi: 10.1289/ehp.1307065. [PubMed: 24508979]

Gryparis A, Paciorek CJ, Zeka A, Schwartz J, Coull BA. Measurement error caused by spatial misalignment in environmental epidemiology. Biostatistics. 2009; 10:258–74. doi:10.1093/biostatistics/kxn033. [PubMed: 18927119]

IOM (Institute of Medicine).. Long-term health consequences of exposure to burn pits in Iraq and Afghanistan. The National Academies Press; Washington, DC: 2011.

Klooga I, Chudnovsky AA, Just AC, Nordio F, Koutrakis P, Coull BA, Lyapustine A, Wang Y, Schwartz J. A new hybrid spatio-temporal model for estimating daily multi-year PM2.5 concentrations across northeastern USA using high resolution aerosol optical depth data. Atmospheric Environment. 2014; 95:581–590. doi:10.1016/j.atmosenv.2014.07.014.

Kloog I, Koutrakis P, Coull BA, Lee H-J, Schwartz J. Assessing temporally and spatially resolved PM2.5 exposures for epidemiological studies using satellite aerosol optical depth measurements. Atmospheric Environment. 2011; 45:6267–6275. doi:10.1016/j.atmosenv.2011.08.066.

Kloog I, Nordio F, Coull BA, Schwartz J. Incorporating local land use regression and satellite aerosol optical depth in a hybrid model of spatiotemporal PM2.5 exposures in the mid-atlantic states. Environ. Sci. Technol. 2012; 46:11913–11921. doi: 10.1021/es302673e. [PubMed: 23013112]

Koutrakis P, Coull BA, Lee H-J, Schwartz J. Assessing temporally and spatially resolved PM2.5 exposures for epidemiological studies using satellite aerosol optical depth measurements. Atmospheric Environment. 2011; 45:6267–6275. doi:10.1016/j.atmosenv.2011.08.066.

Lee H-J, Liu Y, Coull BA, Schwartz J, Koutrakis P. A novel calibration approach of MODIS AOD data to predict PM2.5 concentrations. Atmos. Chem. Phys. 2011; 11:7991–8002. doi:10.5194/acp-11-7991-2011.

Liu Y, Paciorek CJ, Koutrakis P. Estimating regional spatial and temporal variability of PM2.5 concentrations using satellite data, meteorology, and land use information. Environ Health Perspect. 2009; 117:886–892. doi:10.1289/ehp.0800123. [PubMed: 19590678]

Masri SF, Garshick E, Hart J, Bouhamra W, Koutrakis P. Use of visibility measurements to predict PM2.5 exposures in Southwest Asia and Afghanistan. 2015 Manuscript in review.

Morris MJ, Dodson DW, Lucero PF, Haislip GD, Gallup RA, Nicholson KL. Study of active duty military for pulmonary disease related to environmental deployment exposures (STAMPEDE). Ann Am Thorac Soc. 2014; 190:77–84. doi:10.1164/rccm.201402-0372OC.

National Research Council. Review of the department of defense enhanced particulate matter surveillance program report. The National Academies Press. The National Academies Press; Washington, DC: 2010.

NOAA (National Oceanic and Atmospheric Administration). [May 10, 2016] National Climatic Data Center: Climate of Iraq. 2009. http://www.ncdc.noaa.gov/oa/climate/afghan/iraq-narrative.html

Noll KE, Mueller PK, Imada M. Visibility and aerosol concentration in urban air. Atmos Environ. 1967; 2:465–475. doi:1016/0004-6981(68)90040-1.

Roberts AL, Lyall K, Hart JE, Laden F, Just AC, Bobb JF, Koenen KC, Ascherio A, Weisskopf MG. Perinatal air pollutant exposures and autism spectrum disorder in the children of nurses' health study II participants. Environ. Health Perspect. 2013; 121:978–984. doi:10.1289/ehp.1206187. [PubMed: 23816781]

Roop SA, Niven AS, Calvin BE, Bader J, Zacher LL. The prevalence and impact of respiratory symptoms in asthmatics and nonasthmatics during deployment. Mil Med. 2007; 172:1264–1269. doi:10.7205/MILMED.172.12.1264. [PubMed: 18274026]

Smith B, Wong CA, Smith TC, Boyko EJ, Gackstetter GD, Ryan MAK. Newly reported respiratory symptoms and conditions among military personnel deployed to Iraq and Afghanistan: a prospective population-based study. Am J Epidemiol. 2009; 170:1433–1442. doi: 10.1093/aje/kwp287. [PubMed: 19850627]

USEPA (U.S. Environmental Protection Agency). [May 10, 2016] Particulate matter. 2015. http://www.epa.gov/airtrends/pm.html

Waggoner AP, Weiss RE. Preliminary communication: comparison of fine particle mass concentration and light scattering extinction in ambient aerosol. Atmos Environ. 1980; 14:623–62. doi: 10.1016/0004-6981(80)90098-0.

WHO (World Health Organization). [May 10, 2016] Ambient (outdoor) air pollution in cities database. 2014. http://www.who.int/phe/health_topics/outdoorair/databases/cities/en/

WHO (World Health Organization). [May 10, 2016] Air quality guidelines for particulate matter, ozone, nitrogen dioxide and sulfur dioxide.. Global update 2005. 2005. http://apps.who.int/iris/bitstream/10665/69477/1/WHO_SDE_PHE_OEH_06.02_eng.pdf

Yanosky JD, Paciorek CJ, Schwartz J, Laden F, Puett R, Suh HH. Spatio-temporal modeling of chronic PM10 exposure for the Nurses' Health Study. Atmos. Environ. 2008; 42:4047–4062. doi:10.1016/j.atmosenv.2008.01.044.

Implication Statement

This study demonstrates the ability to utilize aerosol optical depth to successfully estimate visibility spatially and temporally in Southwest Asia and Afghanistan. This enables for the estimation of spatially resolved $PM_{2.5}$ concentrations in the region. The ability to characterize $PM_{2.5}$ concentrations in Southwest Asia and Afghanistan is highly important for epidemiologists investigating the relationship between chronic exposure to $PM_{2.5}$ and respiratory diseases among military personnel deployed to the region. This information will better position policy makers to draft meaningful legislation relating to military health.

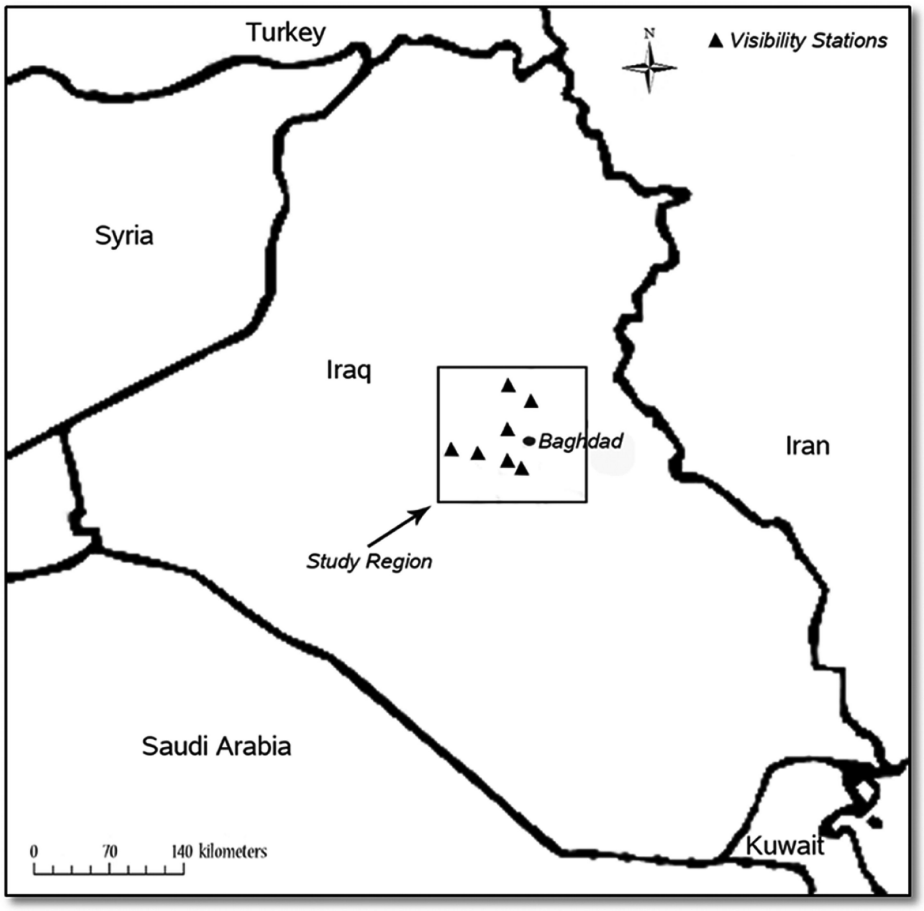

Figure 1.
Map showing visibility monitoring stations in Iraq study region.

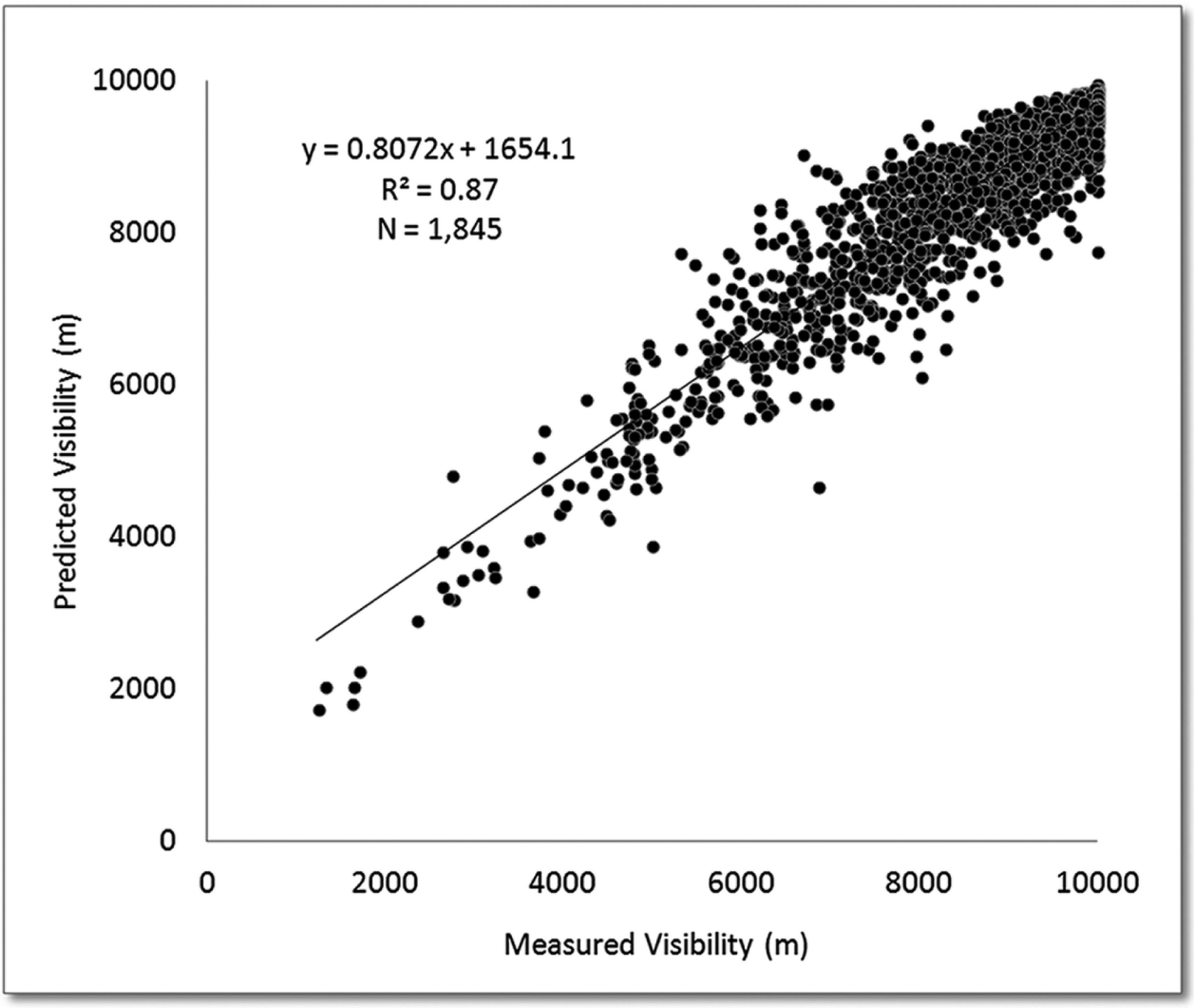

Figure 2.
Relationship between predicted and measured daily average visibility.

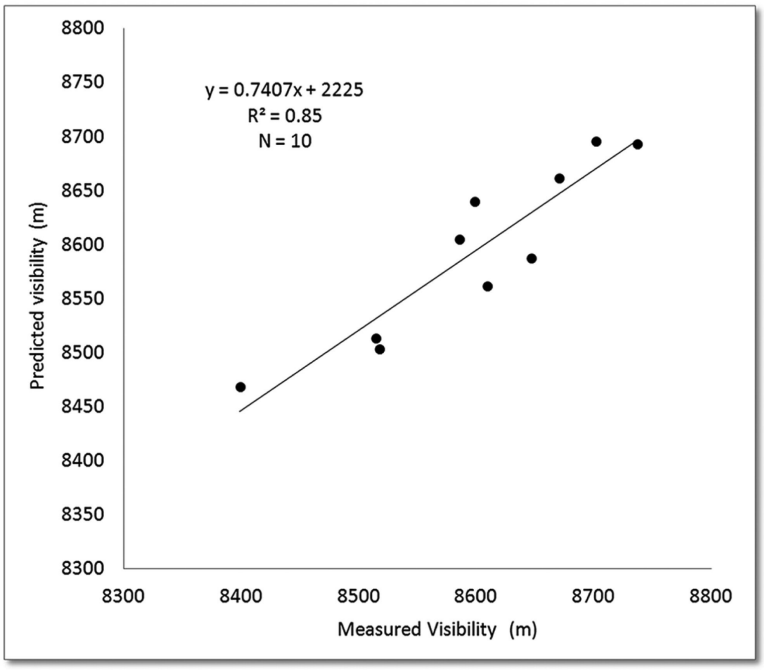

Figure 3.
Plot of predicted versus measured visibility averages for each of 10 CV trials.

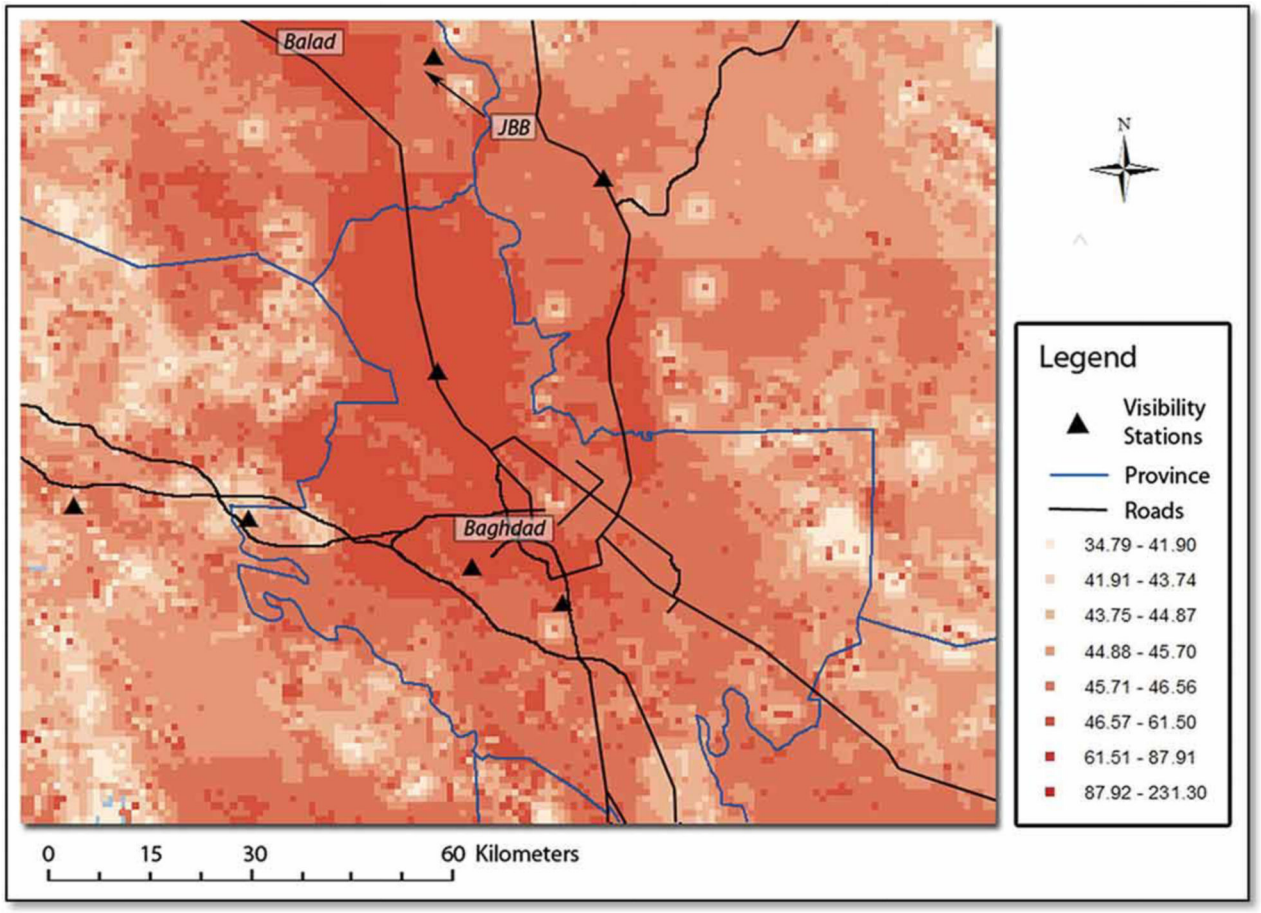

Figure 4.
Spatial pattern of 1×1 km $PM_{2.5}$ predictions averaged over two years (2006-2007).

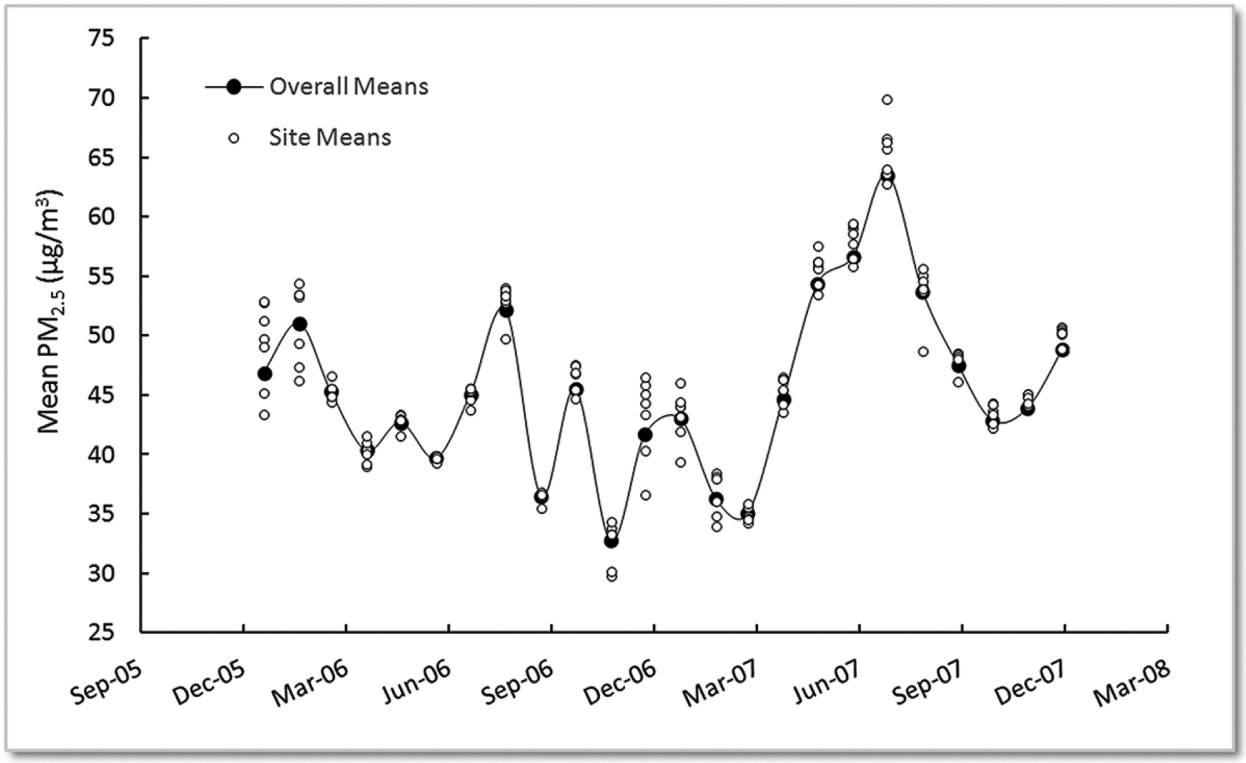

Figure 5.
$PM_{2.5}$ monthly predictions by site and across sites during the study period.

Table 1

Prediction accuracy for 10-fold cross validation (CV) trials of Stage 1 calibration model.

Trial	CV R^2	CV $R^2_{Spatial}$	CV $R^2_{Temporal}$	RMSPE[a] (m)
1	0.83	0.96	0.73	580.5
2	0.67	0.89	0.56	831.8
3	0.71	0.86	0.67	795.6
4	0.76	0.60	0.63	679.4
5	0.74	0.77	0.60	703.6
6	0.67	0.84	0.51	886.5
7	0.76	0.98	0.64	816.2
8	0.63	0.94	0.51	909.3
9	0.64	0.95	0.55	913.3
10	0.71	0.63	0.51	798.2
Mean	0.71	0.87	0.60	790.7

[a]Root of the mean squared prediction errors.

Table 2

Prediction accuracy for 10-fold cross validation (CV) of Stage 3 calibration model.

Site	CV R^2	CV $R^2_{Spatial}$	CV $R^2_{Temporal}$	RMSPE[a] (m)
1	0.82	0.96	0.64	571.6
2	0.85	0.69	0.75	569.8
3	0.87	0.88	0.81	538.9
4	0.80	0.99	0.66	664.5
5	0.91	0.98	0.83	505.4
6	0.83	0.86	0.68	601.2
7	0.84	0.98	0.70	621.8
8	0.78	0.93	0.56	604.9
9	0.85	0.87	0.66	544.6
10	0.90	0.94	0.84	487.3
Mean	0.84	0.91	0.71	580.3

[a]Root of the mean squared prediction errors.